

## Screening of histone deacetylases (HDAC) expression in human prostate cancer reveals distinct class I HDAC profiles between epithelial and stromal cells

D. Waltregny,<sup>1,2</sup> B. North,<sup>3</sup> F. Van Mellaert,<sup>1</sup> J. de Leval,<sup>2</sup> E. Verdin,<sup>3</sup> V. Castronovo<sup>1</sup>

<sup>1</sup>Metastasis Research Laboratory/Center for Experimental Cancer Research and <sup>2</sup>Dept. of Urology, University of Liège, B-4000 Liège, Belgium, <sup>3</sup>Gladstone Institute of Virology and Immunology, University of California, San Francisco, CA 94103, USA



©2004, European Journal of Histochemistry

Histone deacetylases (HDACs) represent a large family of enzymes identified as key regulators of nucleosomal histone acetylation, a major epigenetic event that controls eukaryotic gene transcription. Inappropriate deacetylation mediated by HDACs has been associated with profound alterations in cellular biology. We have thus hypothesized that an altered HDAC expression may favor cancer development/progression. To test this possibility, we have sought to screen the expression profiles of several class I and class II HDACs (HDAC1-8) in DU-145, PC-3 and LNCaP human prostate cancer cell lines as well as in matched malignant and non-malignant prostate tissues by use of real time RT-PCR, immunoblot and immunohistochemistry. All HDAC transcripts tested were detected at various levels in all prostate cancer cell lines and tissue samples analyzed. In prostate tissues, the abundance of HDAC1 protein, which was exclusively expressed in the cell nucleus, was similar in normal and malignant epithelial cells, but was usually lower in stromal cells. Unexpectedly, HDAC8, another class I HDAC, was not detected in epithelial cells but was uniquely expressed in the cytoplasm of stromal cells. HDAC5, a class II HDAC involved in myogenesis, was not detected in the tissues. Altogether, our findings indicate that epithelial and stromal cells exhibit distinct class I HDAC expression profiles, and the abundance of HDAC1 is not altered in human prostate cancer. In addition, our observations are the first to demonstrate the prominently cytosolic distribution of a class I HDAC, HDAC8.

**Key words:** prostate, cancer, histone, deacetylase, expression.

**Correspondence:** David Waltregny, Metastasis Research Laboratory, Pathology Building, Bat. B23, level -1, CHU Sart Tilman Liège, B-4000 Liège 1, Belgium.  
Fax: international +32.4.3662975.  
E-mail: david.waltregny@ulg.ac.be

**Paper accepted on March 16, 2004**

**European Journal of Histochemistry  
2004; vol. 49 issue 3**

Prostate cancer cells exhibit several unique properties that demarcate them from their normal counterparts. Among these peculiarities are increased growth rates, loss of differentiation, escape from cell death pathways and anti-proliferative signals, decreased dependence on exogenous growth factors and release from replicative senescence. Acquisition of these features by malignant prostate epithelial cells requires impairment of normal cellular control mechanisms that result in part from an inappropriate regulation of gene expression. Post-translational modification of nucleosomal histones, which converts regions of chromosomes into transcriptionally active or inactive chromatin, has emerged as an important step in the transcriptional regulation of eukaryotic genes.

The most well investigated post-translational modification of histones is the acetylation of epsilon-amino groups on conserved lysine residues in the amino-terminal tail of the proteins (Megee PC et al., 1990; Grunstein M, 1997). The regulation of histone acetylation levels *in vivo* is a dynamic process under the control of competing enzymes: histone acetyltransferases (HAT) and histone deacetylases (HDAC). Currently, over a dozen cloned HATs have been cloned and, to date, at least 18 different members of the HDAC family have been isolated from mammalian cells (Gray SG et al., 2001; De Ruijter AJ et al., 2003). Most HDACs can function as transcriptional corepressors and are often present in large multi-subunit complexes (Alland L et al., 1997; Nagy L et al., 1997; Knoepfler PS et al., 1999; Koipally J et al., 1999). Interestingly, a number of non-histone proteins, such as the tumor suppressor p53 (Luo J et al., 2001; Vaziri H et al., 2001; Langley E et al., 2002) and the cytoskeleton protein  $\alpha$ -tubulin (Hubbert C et al., 2002), are also substrates for HDACs, which regulate their activity by deacetylation.

HDACs are usually separated into classes on the

basis of their similarity to various yeast HDACs: (i) class I members, including HDAC1, HDAC2, HDAC3, HDAC8, and HDAC11, which are homologous to the yeast Rpd3 protein (Taunton J et al., 1996; Yang WM et al., 1997; Buggy JJ et al., 2000; Hu E et al., 2000; Van den Wyngaert I et al., 2000; Gao L et al., 2002); (ii) class II HDACs, including HDAC4, HDAC5, HDAC6, HDAC7, HDAC9, and HDAC10, which have similarities to yeast Hda1 (Grozinger CM et al., 1999; Kao HY et al., 2000; Zhou X et al., 2001; Fischer DD et al., 2002; Guardiola AR et al., 2002; Kao HY et al., 2002; Tong JJ et al., 2002); and, (iii) NAD-dependent sirtuin (SIRT) proteins, which are homologous to the yeast Sir2 protein (Frye RA, 1999; Imai S et al., 2000; Schwer B et al., 2002). Up to now, 7 human SIRT homologues have been identified. HDAC function is regulated by different mechanisms, including protein-protein interactions, post-translational modification, and sub-cellular localization. Recently, we have shown that the enzymatic activity associated with class II HDAC is dependent on a multiprotein complex containing HDAC3 and N-CoR/SMRT (Fischle W et al., 2002).

The availability of potent histone deacetylase inhibitors has stimulated many studies aimed at testing these new drugs as anticancer agents (Kramer OH et al., 2001). Indeed, these HDAC inhibitors may enable the re-expression of silenced regulatory genes in neoplastic cells, reversing the transformed phenotype (Kwon HJ et al., 1998; Kim YB et al., 1999). Specific HDAC inhibitors, such as trichostatin A (TSA), trapoxin or suberoylanilide hydroxamic acid (SAHA), have been shown to be potent inducers of growth arrest, differentiation, and/or apoptosis of normal and malignant cells (for review, (Cress WD et al., 2000; Marks PA et al., 2000)). In prostate cancer, TSA and several short-chain fatty acids (e.g. butyrates) have triggered growth inhibition and/or apoptosis in androgen-insensitive PC-3 or androgen-sensitive LNCaP human prostate cancer cells (Halgunset J et al., 1988; Walls R et al., 1996; Ellerhorst J et al., 1999; Maier S et al., 2000; Suenaga M et al., 2002; Kuefer R et al., 2004), with concomitant reduction in the levels of telomerase reverse transcriptase mRNA expression (Suenaga M, Soda H et al., 2002). Administration of pyroxamide, SAHA, 2 hydroxamic acid-based hybrid polar compounds with anti-HDAC activity, to nude mice could significantly suppress the growth of CWR22 prostate can-

cer xenografts, without causing detectable toxicity (Butler LM et al., 2000; Butler LM et al., 2001). Similar effects have been obtained with the butyrate analogues isobutyramide and tributyrin in LNCaP and PC-3 xenograft models, respectively (Gleave ME et al., 1998; Kuefer R, Hofer MD et al., 2004). Recently, it has been suggested that HDAC4 nuclear accumulation may coincide with the loss of androgen sensitivity in hormone refractory cancer of the prostate (Halkidou K et al., 2003). Finally, others and we have recently shown that HDAC inhibitors may also have anti-angiogenic properties *in vitro* and *in vivo* (Kim MS et al., 2001; Pili R et al., 2001; Deroanne CF et al., 2002).

Since inappropriate deacetylation mediated by HDACs may lead to as profound cellular biology alterations as changes in cell proliferation, differentiation and apoptosis, one might presume that an altered expression of HDAC enzymes may participate in the development and/or progression of cancer lesions. To investigate this possibility, we have sought to determine the expression profiles of several HDAC members in normal and malignant human prostate cancer. We have first assessed the mRNA expression levels of several class I and class II HDACs (HDAC1-8) in matched normal and malignant human prostate tissues by use of real time RT-PCR. We have then tested by immunoblot and immunohistochemistry several antibodies raised against these various HDACs. For some of them, attempts to obtain specific signals or stainings have remained unsuccessful while antibodies directed against other HDACs have not been available. As a consequence, we have focused our HDAC expression analysis in the normal and malignant prostate on the expression profiles of HDAC1, HDAC5 and HDAC8 enzymes.

## Materials and Methods

### **Cell lines, tissue culture, and reagents**

PC-3, DU-145 and LNCaP human prostate cancer cell lines were purchased from the American Type Culture Collection (Rockville, MD, USA). Cells were routinely grown in RPMI-1640 supplemented with 10% decomplexed fetal bovine serum and 2mM L-glutamine at 37°C in a humidified 95% air/5% CO<sub>2</sub> atmosphere. All tissue culture reagents were obtained from Invitrogen (Merelbeke, Belgium) unless otherwise specified.

## Patients and Tissues

Fresh as well as formalin-fixed paraffin-embedded normal and cancerous prostate tissue samples were obtained from patients who had undergone a radical prostatectomy for clinically localized prostate cancer in the Department of Urology at the University Hospital of Liège, Belgium, during the period from 1996 through 2001. None of the patients included in this study had received preoperative hormonal or radiation therapy. All patients had a clinically confined tumor, classified as stage T1 or T2 NOMO, according to the TNM system (Schröder FH et al., 1992). Absence of regional or distant extension of the tumor was assessed before surgery by chest x-ray, pelvic computed tomography scan, and bone scanning. All patients had undergone a bilateral ilio-obturator lymphadenectomy prior to excision of the prostate gland and histopathological examination of the resected lymph nodes had shown absence of tumor infiltration. The Ethics Committee of the University Hospital of Liège approved the specific protocol used in this study.

## Fresh human prostate tissue harvesting and processing

In order to evaluate HDAC1, HDAC2, HDAC3, HDAC4, HDAC5, HDAC6, HDAC7 and HDAC8 protein and mRNA expression in non-neoplastic and neoplastic prostate tissues from the same patient by use of Western blotting and quantitative RT-PCR, respectively, fresh samples of normal and malignant prostate tissue were harvested from radical prostatectomy specimens according to a previously described method (Wheeler TM et al., 1994). Briefly, tissue samples were taken from the peripheral and transitional zones using a 6- or 8-mm diameter punch biopsy instrument (Stiefel laboratories, Leuven, Belgium). Two one millimeter-thick slices were immediately sectioned from both ends of each fresh cylinder-shaped sample and either included in Tissue-Tek® OCT (Optimum Cut Medium) compound (Miles Inc., West Haven, CT), frozen in liquid nitrogen vapors and stored at  $-80^{\circ}\text{C}$ , or fixed in 10% phosphate buffered formalin overnight, dehydrated in graded alcohols, and paraffin embedded. The remaining cylinder was flash-frozen in liquid nitrogen and then stored at  $-80^{\circ}\text{C}$  for subsequent RNA and protein isolation. Five  $\mu\text{m}$  thick sections were cut from the tissue slices and stained with hematoxylin and eosin. Stained sections were examined under the micro-

scope to determine the presence and extent of areas of normal glandular prostate tissue, prostate intra-epithelial neoplasia (PIN), and adenocarcinoma. Snap-frozen tissue cylinders containing prostate cancer were selected for immunoblot and RT-PCR experiments only when cancer cells areas represented at least 50% of the total surface of the corresponding H&E stained sections.

## Antibodies

Expression of HDAC1 was examined by immunohistochemistry and immunoblot techniques with the use of 3 different anti-HDAC1 sera: (i) a specific anti-HDAC1 serum raised against a peptide corresponding to the predicted C-terminal domain of human HDAC1 (amino acids 467-482) (Emiliani S et al., 1998), (ii) a rabbit polyclonal anti-HDAC1 antibody raised against a peptide corresponding to amino acids 53-482 of mouse HDAC1 (Upstate Biotechnology, Lake Placid, NY, USA), and (iii) a polyclonal anti-HDAC1 antibody raised against a synthetic peptide corresponding to the C-terminus of human HDAC1 (Cell Signaling Technology Beverly, MA, USA). These antibodies are herein referred as Ab1, Ab2, and Ab3, respectively. Expression of HDAC5 and HDAC8 proteins was investigated by immunoblot and immunohistochemistry using commercially available polyclonal anti-HDAC5 (Cell Signaling Technology Beverly, MA, USA) and anti-HDAC8 (N-20) (Santa Cruz Biotech., Inc., Santa Cruz, CA) antibodies, respectively. The anti-HDAC8 antibody was raised against a peptide mapping at the amino terminus of HDAC8 of human origin (Santa Cruz Biotech., Inc., Santa Cruz, CA, USA). RNA and protein extraction. HDAC1-8 protein and transcript expression was examined in normal and malignant human prostate tissue specimens as well as in LNCaP, DU-145 and PC-3 cells. Pulverization of the snap-frozen prostate tissues was performed with the use of a Mikro-Dismembrator U (Braun Biotech., Melsungen, Germany) and generated tissue powder that was immediately processed for protein and RNA extraction. Total RNA was extracted from 20-50 mg of each tissue homogenate with the use of the RNeasy mini kit (Qiagen, Inc., Valencia, CA), according to the manufacturer's protocol. The remaining tissue powder was lysed in 1% sodium dodecylsulfate (SDS) for protein extraction. After rinses in PBS (PBS w/o calcium, magnesium, and sodium bicarbonate), *in vitro* grown human prostate cancer cells (at a confluence of  $\pm 60\%$ ) were

scrapped in presence of either 1% SDS for protein extraction or RNeasy lysis buffer for RNA isolation.

### Immunoblot

Equal amounts of protein extracts (as determined by a bicinchoninic acid determination kit [Pierce Chemical Co., Rockford, IL, USA]) were separated by electrophoresis in 10% SDS-polyacrylamide gels and transferred to polyvinylidene difluoride membranes (Immobilon, Millipore Corp., Bedford, MA, USA), which were stained with Ponceau S (Sigma Chemical Company, St. Louis, MO, USA) to examine the equal protein sample loading and transferring. The membranes were blocked with 5% non-fat dry milk in Tris-buffered saline (20 mM Tris base [pH 7.6], 150 mM NaCl) containing 0.1% Tween-20 (TBS-T), and probed with an anti-HDAC1 (Ab1, Ab2, or Ab3, see 'Antibodies'), anti-HDAC5 or anti-HDAC8 antibody. After washing in TBS-T, membranes were incubated with horseradish peroxidase (HRP)-conjugated secondary antibodies (Bio-Rad Laboratories, Hercules, CA, USA) and developed using an enhanced chemiluminescence detection system (ECL detection kit; Amersham Corp., Arlington Heights, IL), according to the instructions of the manufacturer. Membranes were exposed to Kodak X-Omat AR films, stripped at 60°C for 1 hour in Tris buffer (80 mM, pH 6.7) containing 2% SDS and 0.25 M 2-mercaptoethanol, washed in TBS-T and then reprobed with an anti-cytokeratin 18 (CK18) monoclonal antibody (CY-90, Sigma, MI, USA). The immunoblots were quantitated by densitometric analysis using the NIH Image 1.6.2. software (NIH, Bethesda, MD; <http://rsb.info.nih.gov/nih-image/>).

### Real-time reverse transcription-polymerase Chain reaction (RT-PCR)

#### Reverse Transcription

For cDNA synthesis, 1 µg of total RNA was reverse-transcribed in a 20 µl reaction mixture containing 250 µM of each dNTP, 20 U of RNase inhibitor, 50 U of MuLV Reverse Transcriptase (RT), 2.5 µM Random Hexamers, and 1X buffer (1.5 mM MgCl<sub>2</sub>) (all reagents purchased from PE Applied Biosystems, Foster City, CA, USA). The reaction mix was incubated at 42°C for 45 min and then denatured at 99°C for 5 min. Reactions not containing the RT or omitting the target RNA were used as controls.

#### Primers and probes

Specific primers and probes for the human HDAC1, HDAC2, HDAC3, HDAC4, HDAC5, HDAC6, HDAC7

**Table 1. Sequences of HDAC primers and probes used for Taqman® PCR experiments. Oligonucleotide name Sequence.**

<b>HDAC1 amplicon size: 102 bp</b>	
HDAC1 forward primer	ACCGGGCAACGTTACGAAT
HDAC1 reverse primer	CTATCAAAGGACACGCCAAGTG
HDAC1 hybridization probe	CACCGCTCCAGCATCAGCA
<b>HDAC2 amplicon size: 151 bp</b>	
HDAC2 forward primer	TCATTGAAAATTGACAGCATAGT
HDAC2 reverse primer	CATGGTGATGGTGTGAAGAAG
HDAC2 hybridization probe	CCITTTCCAGCACC AATATCCCTCAAGT
<b>HDAC3 amplicon size: 87 bp</b>	
HDAC3 forward primer	TTGAGTCTGCTCGCGTTACA
HDAC3 reverse primer	CCCAGTTAATGGCAATATCACAGAT
HDAC3 hybridization probe	CTCTGCAAGGAGCAACCCAGCTGAA
<b>HDAC4 amplicon size: 115 bp</b>	
HDAC4 forward primer	AATCTGAACCACTGCATTTCCA
HDAC4 reverse primer	GGTGGTTATAGGAGTCCGACACT
HDAC4 hybridization probe	AACGCAGCACAGTTCCTTGACCAG
<b>HDAC5 amplicon size: 83 bp</b>	
HDAC5 forward primer	TTGAGACGTGGAGTACCTTACAG
HDAC5 reverse primer	GACTAGGACCCATCAGGTGAGAAC
HDAC5 hybridization probe	TGGTGATGCCCATGCCCACG
<b>HDAC6 amplicon size: 127 bp</b>	
HDAC6 forward primer	TGGCTATTGCATGTTCAACCA
HDAC6 reverse primer	GTGCAAGGTGAATGTGTTCTT
HDAC6 hybridization probe	CCCCTATGCTCAACAGAAACACCG
<b>HDAC7 amplicon size: 91 bp</b>	
HDAC7 forward primer	CTCGATTGGAGGAATGAAGCT
HDAC7 reverse primer	CTGGCACAGCGGATGTTTG
HDAC7 hybridization probe	TGTGCTGTCCACCCCAACCCCA
<b>HDAC8 amplicon size: 78 bp</b>	
HDAC8 forward primer	TCCCAGTATGTGAGTATATAGA
HDAC8 reverse primer	GCTTCAATCAAAGAATGCACCAT
HDAC8 hybridization probe	CCTGGCCAAGATCCCAACCG

and HDAC8 genes (Table 1) were designed from sequences available in the GenBank database, using the Primer Express 1.0 Software (PE Applied Biosystems, Foster City, CA, USA). The housekeeping CYCLOPHILIN and 18S rRNA genes (control reagents kit, PE Applied Biosystems, Foster City, CA) were used as endogenous controls to normalize the amount of HDAC transcripts in each reaction. All sets of primers and probes were selected to work under identical cycling conditions. cDNA amplification products using HDAC primers had been previously checked to yield a single band of the expected size after electrophoretic migration in a 2% agarose gel stained with ethidium bromide. HDAC1, HDAC2, HDAC3, HDAC4, HDAC5, HDAC6, HDAC7 and HDAC8 probes were synthesized by PE Applied Biosystems.

### Real-Time PCR

Taqman® PCR was performed on the cDNA samples using an ABI PRISM 7700 Sequence Detector (PE Applied Biosystems, Foster City, CA, USA). The Taqman® PCR Core Reagent kit (PE Applied Biosystems) was used according to the manufacturer's directions with the following modifications: dUTP was replaced by dTTP at the same concentration, and incubation with AmpErase was omitted. For each sample tested, PCR reaction was carried out in a 50 µl volume containing 2 µl of cDNA reaction (equivalent to 100 ng of template RNA) and 2.5 U of AmpliTaq Gold® (PE Applied Biosystems). Oligonucleotide primers and fluorogenic probes were added to a final concentration of 100nM each. After activation of AmpliTaq Gold® for 10 min at 94°C, amplification step consisted of 45 cycles of 94°C for 45 sec, 58°C for 45 sec, and 72°C for 30 sec.

In each experiment, 6 additional reactions with serial dilutions (50X magnitude) of a prostate cancer cell line cDNA as template were performed with each set of HDAC, cyclophilin, or 18S rRNA primers and probes in the same 96 well plate to generate standard curves relating the threshold cycle (CT) to the log input amount of template. All samples were run in triplicates. PCR reactions with samples in which the reverse transcriptase or the target RNA was omitted from the RT reaction did not yield any significant amplification. The relative amounts of HDAC transcripts in each sample were determined using the standard curve method and were normalized to cyclophilin mRNA expression levels, as described in detail in ABI PRISM Sequence Detection System User Bulletin #2 (PE Applied Biosystems) and elsewhere (Fink L et al., 1998). Relative HDAC transcript level in each cell line analyzed was calculated as a ratio between the HDAC mRNA level in the cell line investigated and the HDAC mRNA level in LNCaP cells. Relative HDAC mRNA level in each tumor/normal sample pair was calculated as a ratio between the HDAC mRNA level in the tumor sample and the HDAC mRNA level in the corresponding normal sample. The amplification efficiencies for HDAC1, HDAC5 and HDAC8 transcripts were also calculated. Because HDAC1 and HDAC5 amplification efficiencies were similar (HDAC1/HDAC5 relative efficiency trendline had a slope value of 0.01), HDAC1 and HDAC5 transcript levels could be compared with reasonable accuracy (Signoretti S et al., 2000).

*In situ* detection of HDAC1 and HDAC8 by

immunofluorescence and immunoperoxidase in human non malignant and malignant prostate tissues and cell lines. Immunofluorescence staining was performed using the ABC Vectastain Elite immunoperoxidase kit (Vector Laboratories, Inc., Burlingame, CA, USA) and fluorescein isothiocyanate (FITC)-conjugated tyramine (NEN, Boston, MA, USA) as peroxidase substrate, according to the suppliers' directions. LNCaP, PC-3, and DU-145 cells grown on slides were gently washed with phosphate-buffered saline (PBS) (10 mM sodium phosphate and 0.9% NaCl [pH 7.4]) prior to fixation. Cells and frozen tissue sections were fixed in freshly prepared 2% paraformaldehyde in PBS for 15 min at 4°C. After 3 washes in PBS for 10 min each, the endogenous peroxidase activity was blocked with 0.3% hydrogen peroxide in methanol for 30 min. Following washes in distilled water for 5 min and in PBS for 20 min, cells and tissues were permeabilized with 0.2% Triton-X-100 (Sigma Chemical Co., St Louis, MO, USA) and 1% normal goat (for HDAC1) serum (NGS) or 1% normal rabbit (for HDAC8) serum (NRS) (Vector Lab. Inc., Burlingame, CA, USA) in PBS for 5 min on ice. The slides were then incubated 3 times with NGS or NRS 3% in PBS for 10 min to block the non specific serum-binding sites. Anti-HDAC1 Ab1 antiserum (Emiliani S, Fischle W et al., 1998) at a dilution of 1:200 or anti-HDAC8 Ab at a dilution of 1:200 was applied and incubated for 1 hr, followed by incubation with a biotinylated goat anti-rabbit (HDAC1) or rabbit anti-goat (HDAC8) Ig antibody and the avidin-biotin-peroxidase complex. After each incubation, the slides were washed 3 times with 1% NGS or NRS in PBS for 5 min. Peroxidase activity was developed for 8 min by a solution containing FITC-conjugated tyramine at a concentration of 1:50 in amplification diluent (NEN, Boston, MA, USA). After 3 washes in PBS for 10 minutes, 4,6-diamidino-2-phenylindole (DAPI) 1:100 (15 min) was used to counterstain the slides, which were subsequently washed with PBS for 5 min and mounted with antifading fluorescent mounting medium (DAKO, Carpinteria, CA, USA) for immunofluorescence microscopic examination. Photomicrographs of the slides were taken with a Leica DM microscope equipped with appropriate filter sets. Color photomicrographs were made from these slides under standard conditions to allow comparison in fluorescence intensities. Immunofluorescence staining with the anti-HDAC1 antiserum was assessed in 5 representative prostate cancer tissue specimens and in their corresponding non neo-

plastic samples. Control experiments included omission of anti-HDAC1 or anti-HDAC8 antibody, use of the preimmune serum corresponding to Ab1 as first antibody, and preincubation of anti-HDAC1 or anti-HDAC8 antiserum with a 100 molar excess of the corresponding peptide prior to the antiserum's use in the immunostaining assay (Emiliani S, Fischle W et al., 1998).

HDAC1 and HDAC8 expression in normal and malignant prostate epithelial cells was also assessed using an immunoperoxidase technique. Immunoperoxidase was performed with the use of the ABC Vectastain Elite kit according to the supplier's directions with some modifications. Briefly, 5 $\mu$ m formalin-fixed paraffin-embedded tissue sections were deparaffinized in xylene, rehydrated, and incubated with 0.25% Triton-X-100 in PBS for 10 min. After blocking of the endogenous peroxidase activity with 0.3% hydrogen peroxide in methanol for 30 min, the sections were incubated with a 10mM citrate buffer (pH=6.0) at 95°C for 40 min, allowed to cool down, and then incubated with 1% normal goat (HDAC1) or swine (HDAC8) serum in PBS for 30 min to block the nonspecific serum-binding sites. Anti-HDAC1 Ab1 at a dilution of 1:1000, anti-HDAC1 Ab2 at a dilution of 1:100, or anti-HDAC8 Ab at a dilution of 1:200 were applied and incubated overnight at 4°C, followed by biotinylated goat anti-rabbit (HDAC1) or swine anti-goat (HDAC8) Ig antibody and the avidin-biotin-peroxidase complex. Slides were washed three times with PBS after each incubation. Peroxidase activity was developed by a solution of 4 mg of 3-3' diaminobenzidine tetrahydrochloride (DAB) (Vel, Leuven, Belgium) dissolved in 10 ml of PBS and 0.03% H<sub>2</sub>O<sub>2</sub>. The DAB solution was filtered and applied to the sections for 4 minutes. Finally, Carazzi's hematoxylin was used to counterstain the slides that were then dehydrated and mounted. Immunoperoxidase staining was performed on 24 prostate cancer sections also containing non malignant prostate glands. These 24 samples were selected according to the Gleason score of the lesions (Gleason DF et al., 1974): score 4 (grade 2+2, n=4), score 5 (grade 2+3, n=4), score 6 (grade 3+3, n=4), score 7 (grade 3+4, n=4), score 8 (grade 3+5, n=1; grade 4+4, n=3), and score 9 (grade 4+5, n=4).

### **Statistical analysis**

The Student t-test and the ANOVA test were used to assess whether pathologic stage and Gleason score, respectively, were significantly associated with

tumor to normal HDAC1 mRNA and protein ratios. The ANOVA test was also used to determine whether tumor/normal HDAC protein ratios significantly correlated with tumor/normal HDAC mRNA or CK18 protein ratios. These statistical tests were two-tailed, and a p value <0.05 was considered statistically significant. The analyses were performed with the Statview II Version 4.2 software (Abacus Concepts Inc., CA, USA).

### **Results**

Expression of class I and class II HDAC transcripts in human prostate cancer cells lines and tissues. Real time RT-PCR experiments were carried out to assess the relative abundance of HDAC1, HDAC2, HDAC3, HDAC4, HDAC5, HDAC6, HDAC7, and HDAC8 transcripts in total RNA extracts from DU-145, PC-3 and LNCaP human prostate cancer cells. The relative levels of HDAC1-8 transcripts in DU-145, PC-3, and LNCaP cells were arbitrarily compared to those obtained in LNCaP cells. As shown in Figure 1A, all HDAC transcripts tested were detected in the 3 cell lines. Interestingly, the HDAC mRNA expression profiles of PC-3 and LNCaP cells were fairly similar with only slight variability, while the HDAC mRNA profile of DU-145 cells was more distinct. Indeed, HDAC3, HDAC4, HDAC5, and HDAC7 mRNA expression levels were at least twofold higher in these latter cells.

The relative levels of HDAC1-8 expression at the transcript level were next determined in total RNA extracts from human prostate cancer tissues and their corresponding normal counterpart. The relative abundance of each HDAC transcript in the tumor/normal sample pairs analyzed was calculated as a ratio between the HDAC transcript level in the tumor sample and the HDAC transcript level in the corresponding normal sample. The results obtained are shown in Figure 1B. In total, 16 tumor/normal prostate tissue pairs were screened for HDAC1 mRNA expression. The abundance of HDAC1 transcripts, normalized to the abundance of cyclophilin A mRNA, was equivalent in most of the matched prostate tumor and normal samples. Indeed, the HDAC1 mRNA ratios ranged between 0.75 and 1.25 in 12 of the 16 pairs tested (75%). Mean tumor/normal HDAC1 mRNA ratio for all sample pairs analyzed was  $0.9 \pm 0.19$  (median = 0.83; range = 0.64-1.41). Similar results were obtained when 18S rRNA was used as endogenous normaliz-

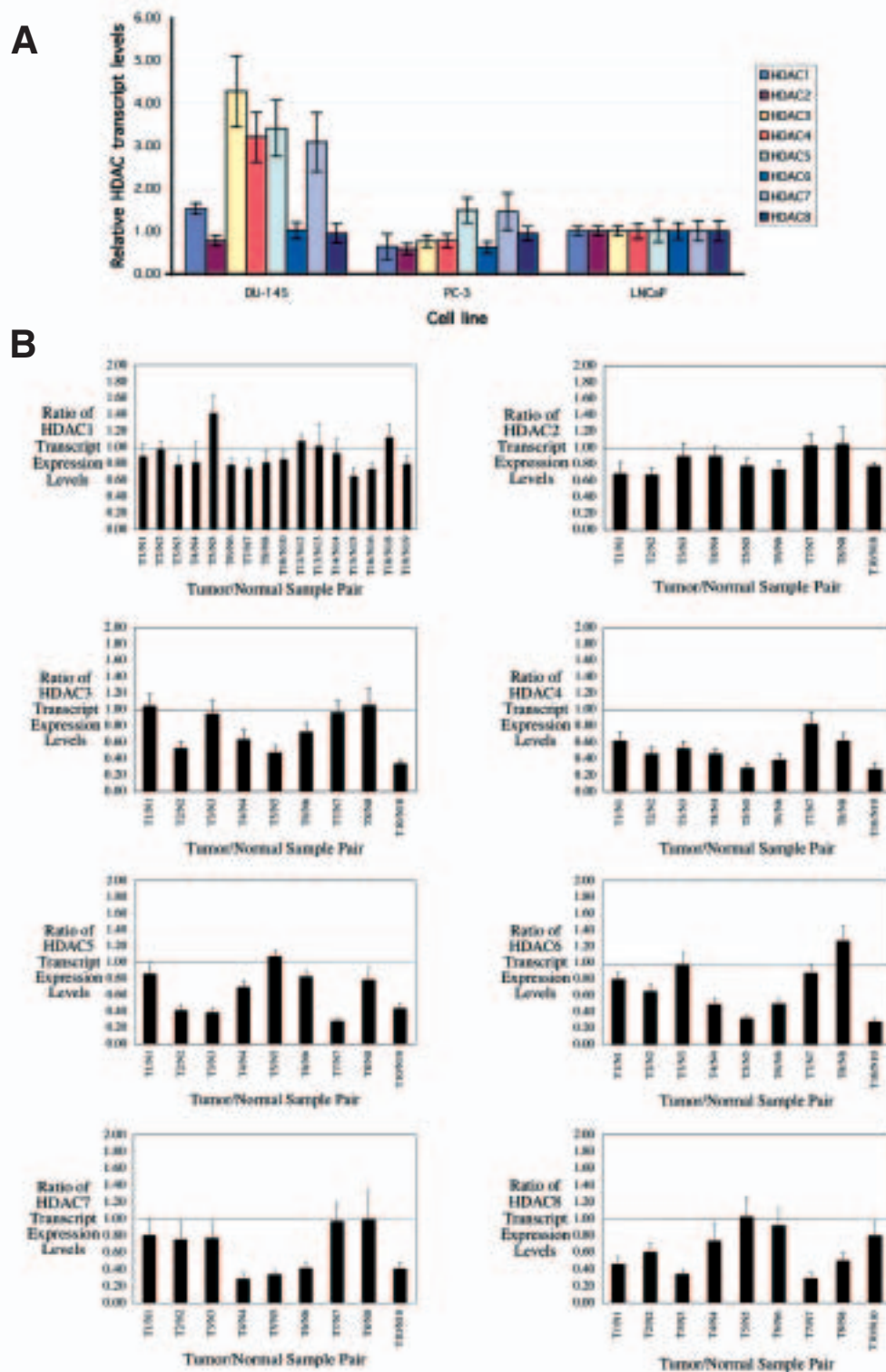


**Figure 1.** A) Analysis of HDAC1, HDAC2, HDAC3, HDAC4, HDAC5, HDAC6, HDAC7 and HDAC8 transcript levels by Taqman® Real-Time RT-PCR in DU-145, PC-3 and LNCaP cells, as described in Materials and Methods. The specific human HDAC primers and probes used in the PCR reactions are shown in Table 2. The relative amounts of HDAC transcripts in each cell line were determined using the standard curve method and were normalized to cyclophilin A mRNA levels. Relative HDAC transcript level in each cell line was calculated as a ratio between the HDAC mRNA level in the cell line and the HDAC mRNA level in LNCaP cells. Samples were run in triplicates and error bars represent standard deviations. B) Prostate cancer and corresponding normal prostate tissues were harvested from radical prostatectomy specimens, as described in Materials and Methods. Total RNA was extracted from each tumor (T) and matched normal (N) sample. One  $\mu\text{g}$  of total RNA per sample was reverse-transcribed and one-tenth of each RT reaction was subjected to Taqman® Real-Time PCR amplification. The relative amounts of HDAC transcripts in each sample were determined using the standard curve method and were normalized to cyclophilin A mRNA expression levels. Relative HDAC mRNA level in each tumor/normal sample pair was calculated as a ratio between HDAC mRNA level in the tumor sample and HDAC mRNA level in the corresponding normal sample. Error bars stand for standard deviation of the ratios.

er (*data not shown*). Likewise HDAC1 transcript levels, the abundance of HDAC2 transcripts was pretty similar in 9 matched prostate tumor and corresponding normal samples analyzed. The HDAC2 mRNA ratios ranged between 0.75 and 1.25 in 7 of the 9 pairs tested (77.8%). Mean tumor/normal HDAC2 mRNA ratio for all sample pairs analyzed was  $0.83 \pm 0.14$  (median = 0.78; range = 0.67-1.04). The tumor/normal HDAC3, HDAC4, HDAC5, HDAC6, HDAC7, and HDAC8 mRNA ratios were also assessed in the same 9 tissue sample pairs. As shown in Figure 1B, the tumor/normal transcript ratios for these HDACs were distinctly more variable. Indeed, the tumor/normal transcript ratios for HDAC3, HDAC4, HDAC5, HDAC6, HDAC7, and HDAC8 were  $<0.5$  in 2, 5, 4, 4, 4, and 4 of the 9 sample pairs analyzed, respectively. None of the tumor/normal mRNA ratios for these HDACs was  $> 1.25$ .

We then attempted to investigate the protein expression levels of HDAC1-8 by immunoblot, immunocytochemistry, and immunohistochemistry. For these experiments, we have utilized various specific anti-HDAC antibodies. However, we were able to obtain appropriate and specific signals/stainings only for HDAC1, HDAC5, and HDAC8 enzymes.

### **Expression of HDAC1 protein in human prostate cancer cell lines and tissues**

Immunoblotting performed on total protein extracts from DU-145, PC-3 and LNCaP cells showed the presence of an expected 60 kD band corresponding to HDAC1 (Figure 2A). Higher levels of HDAC1 were detected in LNCaP cells than in DU-145 and PC-3 cells. Similar patterns of HDAC1 abundance in the 3 cell lines were obtained with the 3 different anti-HDAC1 antibodies used (*data not shown*). Immunocytofluorescence experiments, with the use of anti-HDAC1 Ab1, showed that the enzyme was exclusively detected in the nucleus of all DU-145, PC-3 and LNCaP cells grown on glass slides (Figure 2B). Control experiments in which the anti-HDAC1 antiserum was preincubated with a molar excess of the corresponding peptide completely abolished the labeling (*data not shown*). Similarly, no specific staining was observed when the preimmune serum was used or when the primary antibody was replaced with PBS in the immunofluorescence procedure (*data not shown*).

To search for HDAC1 expression in human prostate cancer tissues, we first performed immunoblots on total protein extracts prepared

**Table 2. Pathologic characteristics of 24 prostate cancer samples obtained from radical prostatectomy specimens.**

Sample	Gleason score	Pathologic stage
T1	6	pT2B
T2	6	pT3A
T3	6	pT3B
T4	6	pT2B
T5	8	pT3A
T6	7	pT2B
T7	6	pT3B
T8	7	pT2B
T9	5	pT3A
T10	6	pT3B
T11	6	pT3A
T12	6	pT3A
T13	6	pT3A
T14	6	pT2B
T15	7	pT2B
T16	5	pT3A
T17	6	pT2B
T18	6	pT3A
T19	6	pT3A
T20	6	pT3B
T21	7	pT3A
T22	6	pT2B
T23	7	pT3A
T24	6	pT2B

from prostate tissue cylinders obtained as described in *Design and Methods*. We evaluated HDAC1 expression in prostate cancer specimens and corresponding normal tissue samples from 20 radical prostatectomies. The pathological stage and the Gleason score of the lesions analyzed are detailed in Table 2.

Immunoblotting experiments were carried out first with the use of 5 different tumor/normal pairs and either Ab1 or Ab3; similar patterns of HDAC1 expression were observed (*data not shown*). A 60 kD band corresponding to HDAC1 was obtained in all 20 tissue samples tested. Figure 3 shows the abundance of HDAC1 in the matched malignant and non malignant prostate specimens from each patient. In 15 out of the 20 cases tested (75%), prostate cancer lesions were found to express higher amounts of the enzyme than the corresponding non-malignant counterpart. Mean tumor/normal HDAC1 ratio for the entire set of tissue pairs was  $1.63 \pm 1.12$  (median = 1.25; range = 0.61-4.23). In 5 sample pairs, HDAC1 tumor/normal ratio was  $\geq 2$ . No significant association was found between tumor/normal HDAC1 protein ratio and either the pathologic stage (Student t-test,  $p=0.64$ ) or the Gleason score of the lesions (ANOVA test,  $p=0.58$ ).

Because of the well-known heterogeneity of prostate cancer lesions and since it is virtually

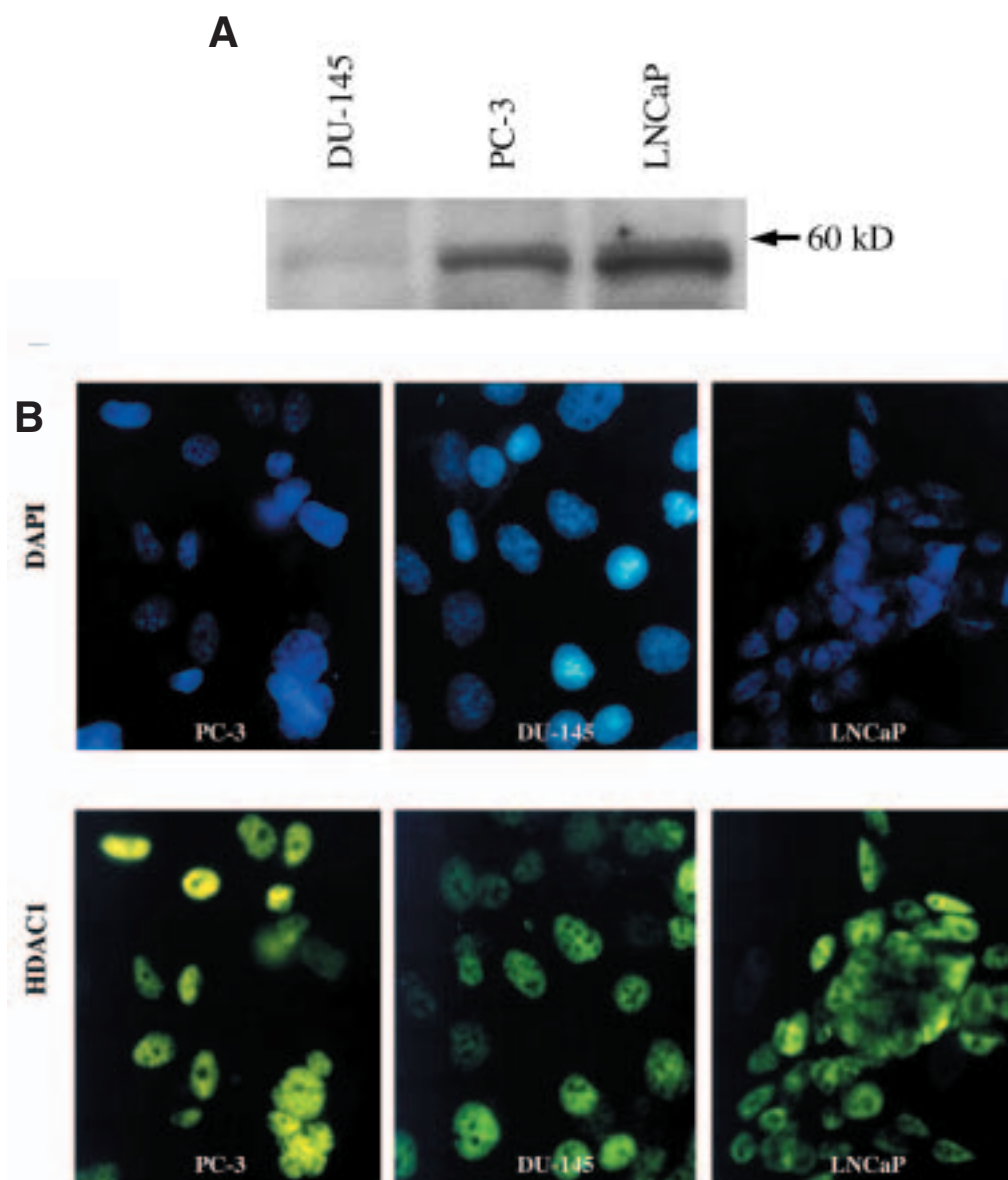


**Figure 2.** A) Protein lysates (30 $\mu$ g per lane) from human DU-145, PC-3, and LNCaP prostate cancer cells were subjected to immunoblot analysis of HDAC1 expression, as described in Materials and Methods. B) Analysis of HDAC1 expression by immunofluorescence using an anti-HDAC1 antibody (Emiliani S, Fischle W et al., 1998) in DU-145, PC-3, and LNCaP cells. Cell nuclei were counterstained with DAPI.

impossible to obtain 100% pure prostate cancer tissues (not contaminated with non malignant glands), we examined the expression of HDAC1 protein at the cellular level using immunofluorescence staining performed on frozen tissue sections bearing prostate cancer. In order to compare the level of nuclear HDAC1 expression in all the cells present in the samples, the nuclei were counterstained with DAPI. HDAC1 expression was found to be exclusively expressed in the nucleus of non-

malignant and malignant epithelial cells (Figure 4 A and B). In all 5 samples examined, nuclear fluorescence intensity appeared to be equivalent in cancer cells and in non-malignant epithelial cells.

We extended our analysis of HDAC1 protein expression to a series of paraffin-embedded prostate cancer lesions with various levels of differentiation using an immunoperoxidase technique. Sections from 24 prostate tissues containing both malignant and non-malignant prostate epithelial

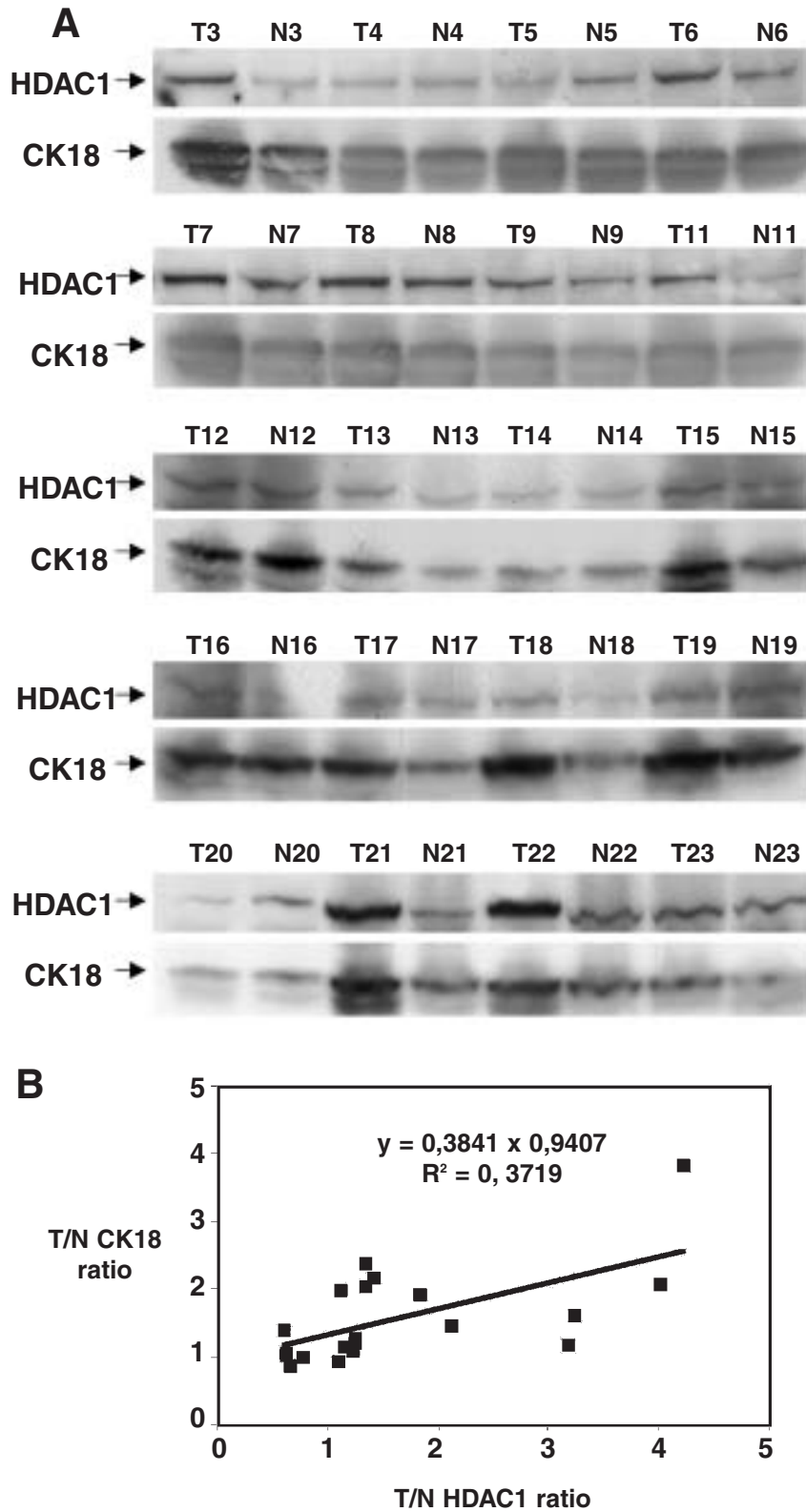
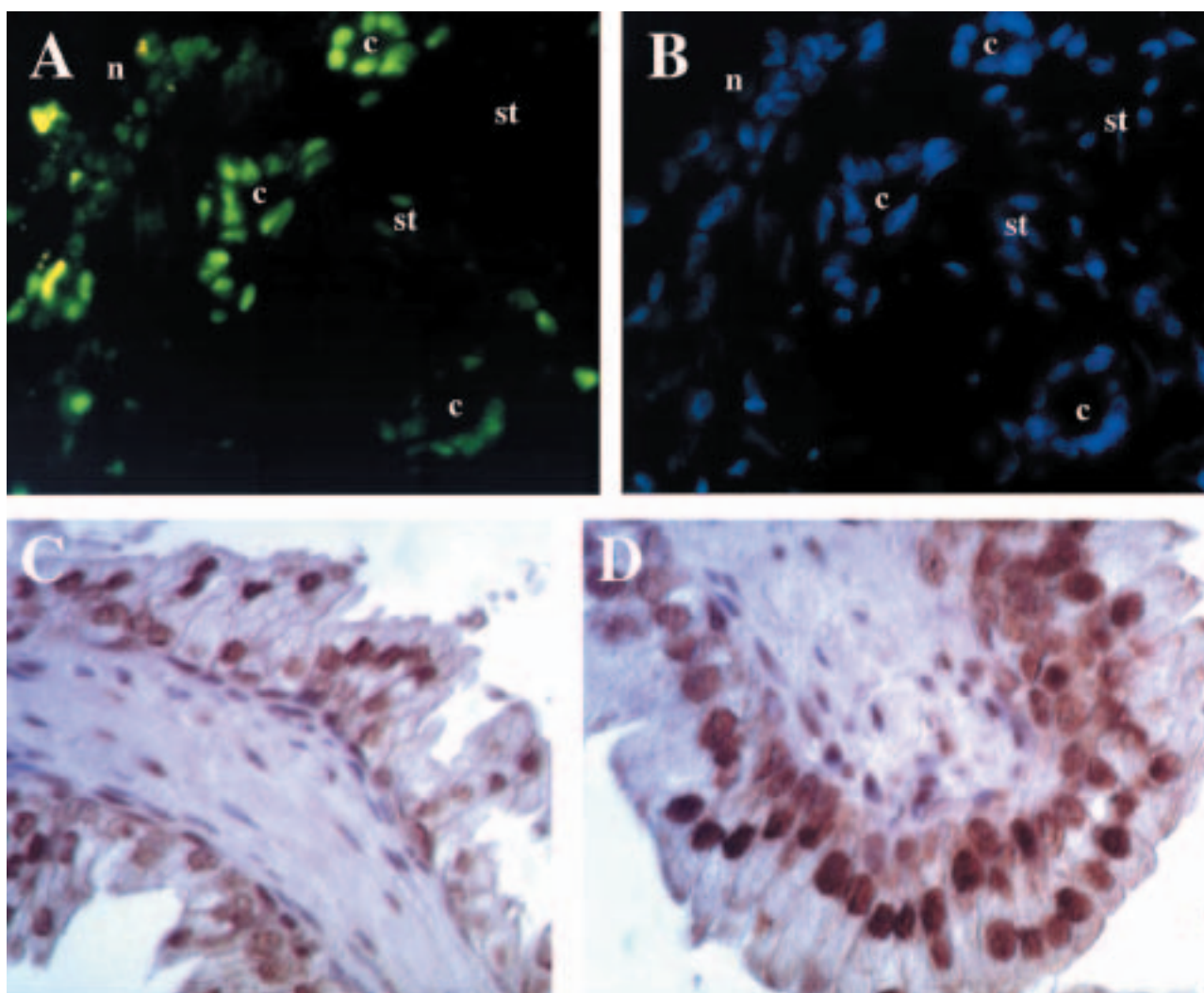


Figure 3. A) Prostate cancer and corresponding normal prostate tissues were harvested from radical prostatectomy specimens, as described in Design and Methods. Total proteins were isolated from each tumor (T) and matched (N) normal sample. Protein lysates (30µg per sample) were subjected to Western blot analysis of HDAC1 and cytokeratin 18 (CK18) expression. Ponceau S staining of the membranes showed equal protein sample loading and transferring (*data not shown*). B) Tumor/normal ratios of HDAC1 and CK18 protein levels were determined as described in Materials and Methods. T/N ratios of HDAC1 expression were plotted against T/N ratios of CK18 abundance and the linear regression obtained with these two variables was calculated using a statistical software. The equation of the regression is indicated in the graph.



**Figure 4.** A) HDAC1 expression was analyzed in prostate cancer-bearing tissue sections using an immunofluorescence technique, as described in Materials and Methods. Expression of HDAC1 in the nucleus of Gleason score 6 prostate cancer cells (c) adjacent to normal epithelial cells (n) and stromal cells (st). B) The nuclei of the same cells as in A) were counterstained with DAPI. C and D) Expression of HDAC1 by immunoperoxidase in epithelial cells from normal prostate glands and underlying stromal cells. Tissue sections were counterstained with hematoxylin. Original Magnification: A and B: x400, C and D: x630.

cells were immunostained with anti-HDAC1 Ab2 antibody. Anti-HDAC1 immunoreactivity was detected in the nucleus of all normal and malignant epithelial cells and no difference in staining intensity was observed between normal and cancerous epithelial cells (Figure 5, panels A through D). The intensity of anti-HDAC1 nuclear reactivity in the tumor cells was not altered by the level of differentiation of the cancer lesions, expressed as the Gleason score (Figures 5 A,B,F,G and H). Similar results were obtained with the use of anti-HDAC1 Ab1 antibody.

Anti-HDAC1 labeling was detected in both basal and secretory epithelial cells from normal prostate glands (Figure 4 C and D, Figure 5 C and D), as

well as in endothelial (Figure 5 E) and inflammatory (*data not shown*) cells. Both immunofluorescence and immunoperoxidase experiments showed that most prostate stromal cells usually exhibited a low or no detectable level of nuclear HDAC1 expression (Figure 4). Since HDAC1 nuclear abundance was higher in epithelial than in stromal cells, we hypothesized that the increased expression of HDAC1 in tumor samples, as determined by immunoblot, was the result of an increased proportion of epithelial cells in the malignant samples as compared with their normal counterpart. Immunoblot experiments using an antibody directed against cytokeratin 18 (CK18), a specific epithelial marker, showed that CK18 expression levels

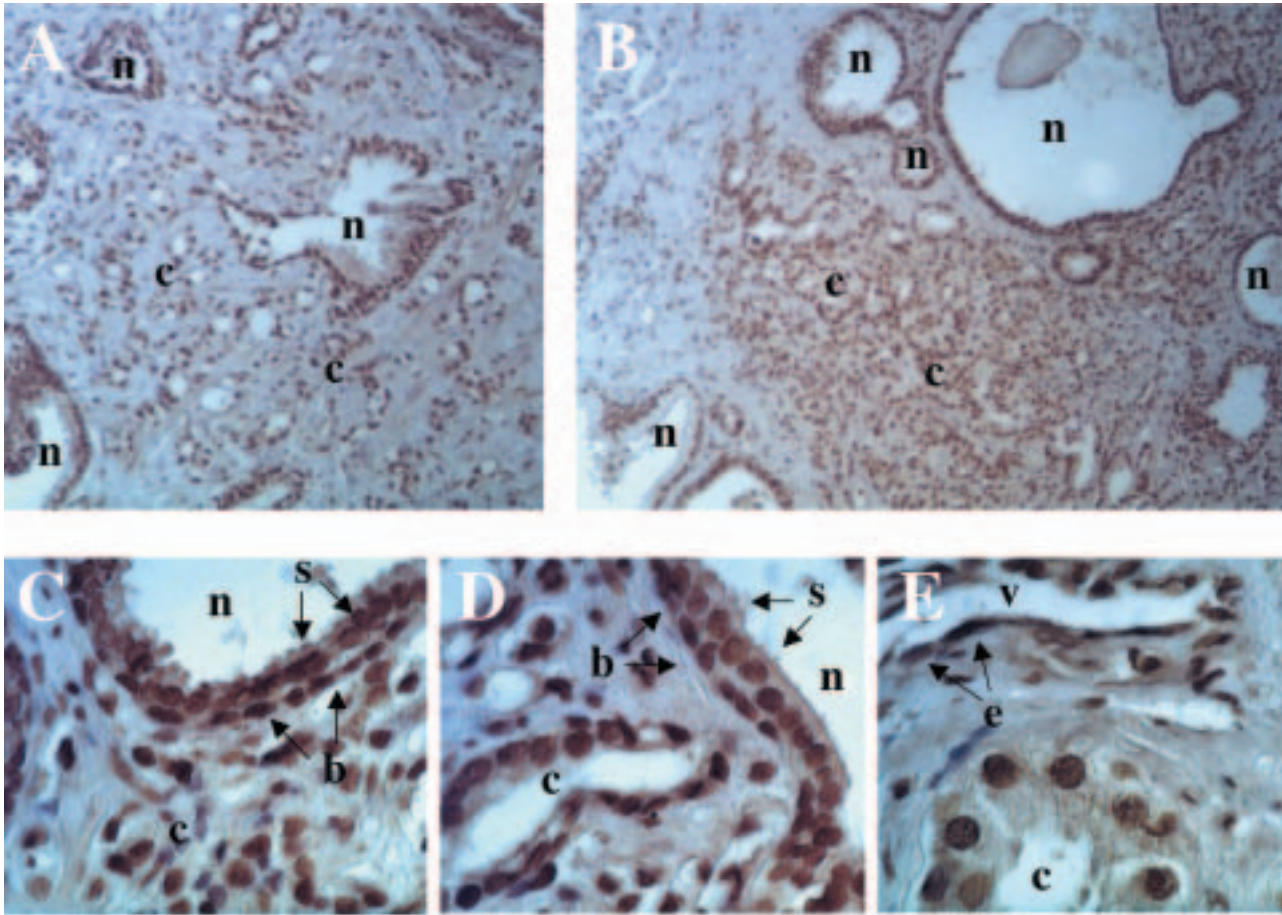


**Figure 5.** HDAC1 expression was analyzed in prostate cancer-bearing tissue sections using an immunoperoxidase technique, as described in Materials and Methods. A) Nuclear detection of HDAC1 in Gleason score 6 prostate adenocarcinoma cells (c) and adjacent non malignant glands (n). B) Nuclear expression of HDAC1 in Gleason score 7 prostate cancer cells and adjacent normal glands. C) Expression of HDAC1 in Gleason score 9 prostate cancer cells and in epithelial secretory (s) and basal (b) cells from adjacent normal glands. D) Detection of HDAC1 in the nucleus of Gleason score 6 prostate cancer cells and adjacent epithelial cells from normal glands. E) Detection of nuclear HDAC1 in endothelial cells (e) of a small blood vessel next to Gleason score 6 prostate cancer cells. F, G, and H) Nuclear detection of HDAC1 in Gleason score 5, 6 and 9 prostate cancer cells, respectively (c = cancer glands/cells). Tissue sections were counterstained with hematoxylin. Original Magnification: A and B: x200, C through E, x630, F through H: x400.

were usually higher in the tumor samples than in the matched normal samples (Figure 3A). Mean T/N CK18 ratio was  $1.58 \pm 0.71$  (median = 1.33; range = 0.87-3.82). Tumor/normal CK18 ratios closely paralleled tumor/normal HDAC1 ratios (ANOVA test,  $p=0.004$ ) (Figure 3B).

Expression of HDAC8 protein in human prostate cancer cell lines and tissues. A unique band at  $\pm 45$ kD was observed in the 3 prostate cancer cell lines tested for HDAC8 expression by immunoblot (Figure 6A). The abundance of HDAC8 protein was higher in DU-145 and PC-3 cells than in LNCaP cells. Immunoblot analysis of HDAC8 expression levels in the human prostate tissues revealed that the abundance of the enzyme was usually lower in the cancer samples than in the corresponding normal ones (Figure 6B). Mean T/N HDAC8 protein

ratio for all 13 sample pairs analyzed was  $0.76 \pm 0.14$  (median = 0.75; range = 0.52-1.01). HDAC8 transcript levels were also decreased in most tumor samples as compared with the matching normal samples, with a mean T/N HDAC8 mRNA ratio of  $0.63 \pm 0.26$  (median = 0.60; range = 0.29-1.02) (Figure 1B). T/N HDAC8 protein ratios were significantly correlated with T/N HDAC8 mRNA ratios (ANOVA test;  $p=0.035$ ).

We next examined the expression of HDAC8 protein at the cellular level using immunofluorescence staining performed on frozen prostate tissue sections. HDAC8 expression was found to be mainly expressed in the cytoplasm of stromal prostate cells (Figure 7 A through D). In all 5 samples examined, no anti-HDAC8 immunostaining was detected in normal or malignant epithelial prostate cells.

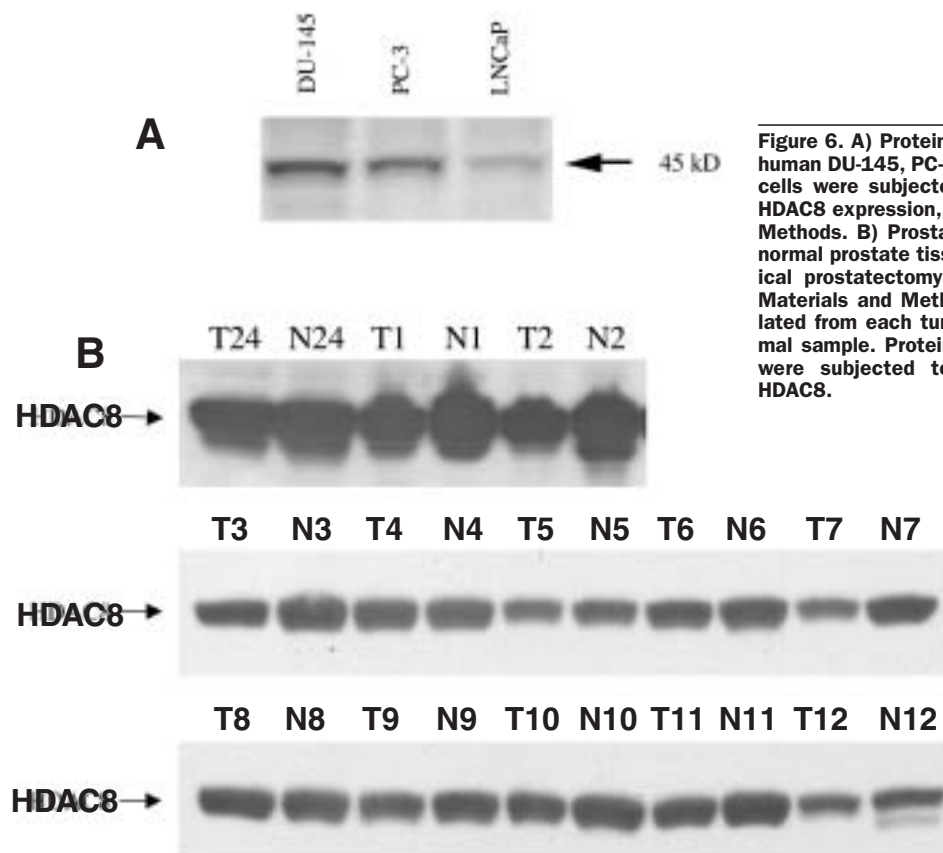


**Figure 6.** A) Protein lysates (30 $\mu$ g per lane) from human DU-145, PC-3, and LNCaP prostate cancer cells were subjected to immunoblot analysis of HDAC8 expression, as described in Materials and Methods. B) Prostate cancer and corresponding normal prostate tissues were harvested from radical prostatectomy specimens, as described in Materials and Methods. Total proteins were isolated from each tumor (T) and matched (N) normal sample. Protein lysates (30  $\mu$ g per sample) were subjected to Western blot analysis of HDAC8.

HDAC8 protein expression was further analyzed by immunoperoxidase staining in the series of 24 paraffin-embedded prostate tissues bearing cancer lesions with various levels of differentiation. Pre-incubation of the anti-HDAC8 antibody with the corresponding peptide completely abolished the immunostaining (Figures 7 E and F). Anti-HDAC8 immunoreactivity was not detected in the normal or malignant epithelial cells in any of the cases analyzed (Figure 7 G and H). HDAC8 protein was expressed by most stromal cells either adjacent to normal glands or intermingled with cancer glands or cells.

Expression of HDAC5 protein in human prostate cancer cell lines and tissues. A unique band at  $\pm$  165kD was observed in all 3 prostate cancer cell lines tested for HDAC5 expression by immunoblot (Figure 8A). The pattern of HDAC5 protein expression in these cells was similar to that of HDAC8 expression, with amounts of HDAC5 protein in DU-145 > PC-3 > LNCaP cells. No HDAC5 expression was detected in any of the normal or malignant prostate tissues tested by immunoblot (Figure 8B), even after prolonged exposure of the membranes.

The relative abundance of HDAC1 and HDAC5 transcripts was compared in the non-malignant prostate tissues using real-time RT-PCR. The mean threshold cycle (CT) for HDAC5 amplification was substantially higher than the mean CT for HDAC1 (24.5 versus 19.8, respectively, when 100 ng of RNA were used as template). Thus, it could be estimated that HDAC5 transcripts were 20 times less abundant than HDAC1 transcripts in these tissues.

## Discussion

Epigenetic mechanisms, including histone acetylation/deacetylation, may be an important driving force for critical changes in gene expression that are responsible for the development/progression of prostate cancers (Rennie PS et al., 1998). Deacetylation of histone proteins can be achieved by a number of HDACs. Most of them act as transcriptional co-repressors yet the specific roles of each of these enzymes in cell biology remains to be unveiled. Although HDACs appear to play a crucial role in carcinogenesis, little is known about the regulation of their expression in normal or neoplastic

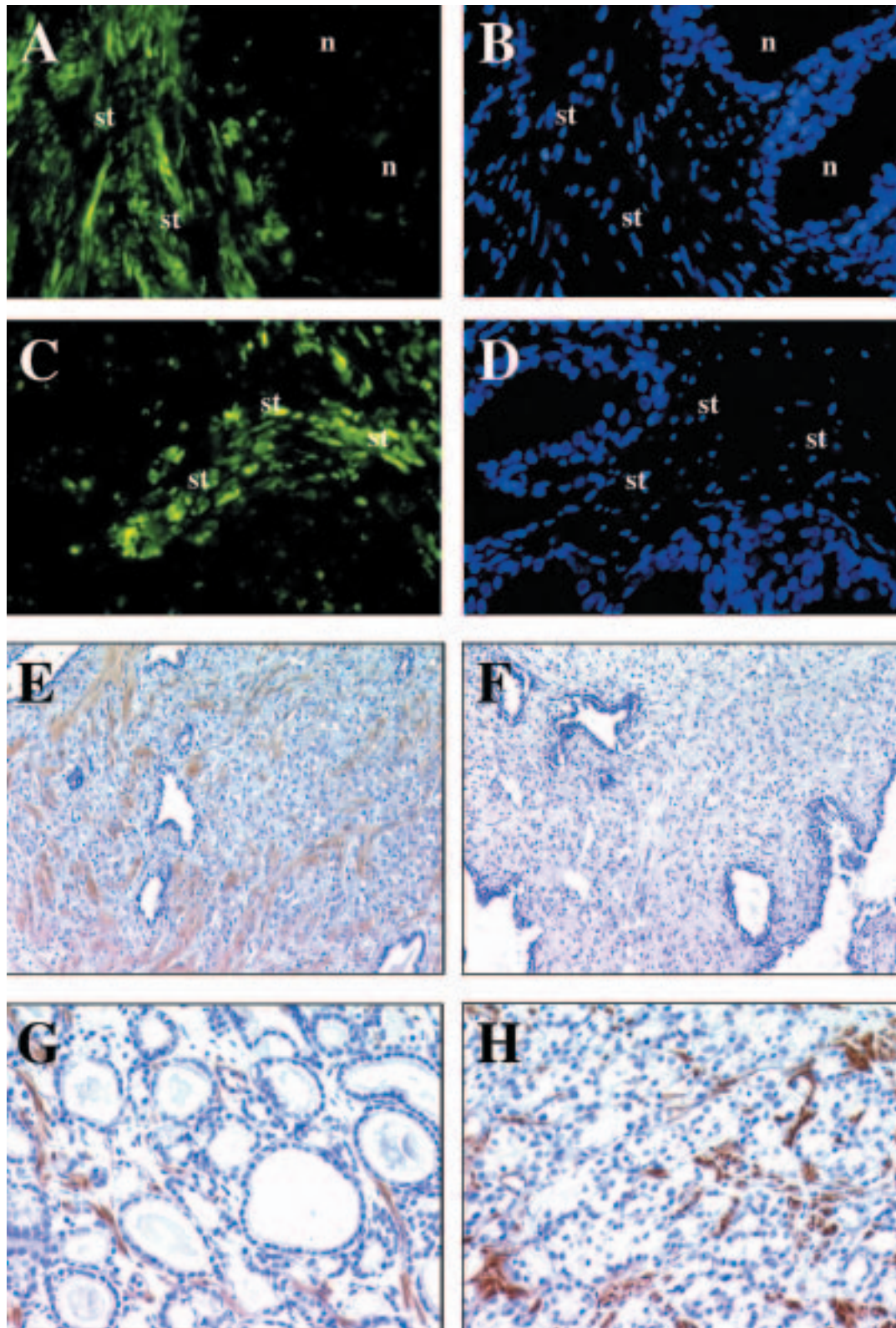


**Figure 7.** A and C) HDAC8 expression was analyzed in prostate tissue sections using an immunofluorescence technique, as described in Materials and Methods. Expression of HDAC8 in the cytoplasm of prostate stromal cells (c) adjacent to normal prostatic epithelium (n). B and D) The nuclei of the same cells as in A) and C) were counterstained with DAPI. E) Expression of HDAC8 by immunoperoxidase in prostate stromal cells adjacent to normal prostate glands and prostate cancer cells. F) Complete abolishment of HDAC8 expression in prostate stromal cells when anti-HDAC8 antibody is preincubated with 100x molar excess of the corresponding peptide. G) Expression of HDAC8 in prostate stromal cells intermingled with well differentiated (Gleason score 4) prostate cancer glands. H) Expression of HDAC8 in prostate stromal cells adjacent to poorly differentiated (Gleason score 9) prostate cancer cells. Tissue sections were counterstained with hematoxylin. Original Magnification: A through D: x400, E and F: x200, G and H: x400.

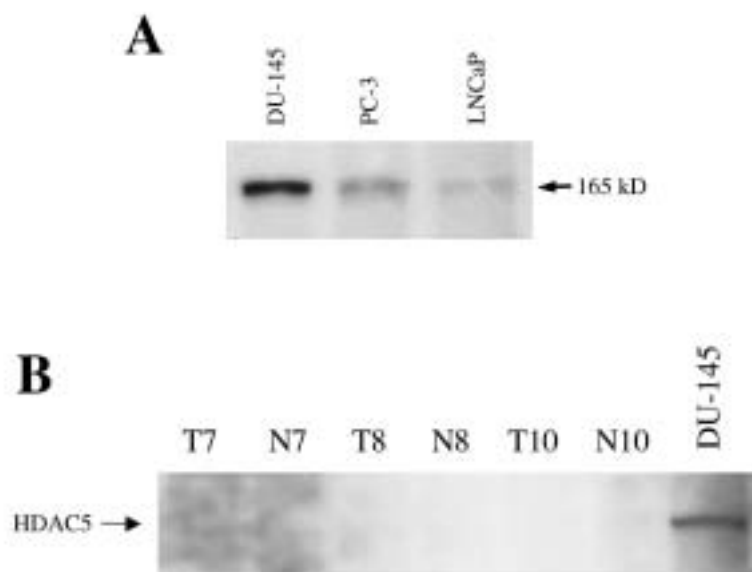


**Figure 8.** A) Protein lysates (30 $\mu$ g per lane) from human DU-145, PC-3, and LNCaP prostate cancer cells were subjected to immunoblot analysis of HDAC5 expression, as described in Materials and Methods. B) Prostate cancer and corresponding normal prostate tissues were harvested from radical prostatectomy specimens, as described in Materials and Methods. Total proteins were isolated from each tumor (T) and matched (N) normal sample. Protein lysates (30  $\mu$ g per sample) were subjected to Western blot analysis of HDAC5.

mammalian cells. It has been reported that the levels of HDAC1, HDAC2, HDAC3, HDAC5 and HDAC6 transcripts in various human and murine cancer cells can be significantly up-regulated by TSA or butyrate treatment (Gray SG et al., 1998; Verdell A et al., 1999; Dangond F et al., 2001). Several studies have also pointed to a possible post-transcriptional regulation of HDAC1 expression (Bartl S et al., 1997), possibly involving the proteasome pathway of targeted protein degradation (Zhou Q et al., 2000).

In this study, we initially searched for the transcript expression profiles of several class I (HDAC1, HDAC2, HDAC3 and HDAC8) and class II HDACs (HDAC4, HDAC5, HDAC6 and HDAC7) in normal and malignant human prostate tissues and cell lines. The results of our real time RT-PCR experiments showed that all HDAC transcripts analyzed were expressed in DU-145, PC-3 and LNCaP human prostate cancer cell lines. Interestingly, the relative levels of HDAC3, HDAC4, HDAC5, and HDAC7 transcripts were substantially higher in DU-145 cells than in PC-3 and LNCaP cells, which exhibited similar HDAC transcript expression profiles. Whether these differences in HDAC mRNA expression profiles may have an impact on the biological activities of these cells needs to be further addressed. HDAC1-8 transcripts were also detected at various levels in all normal and cancerous human prostate tissues tested. No overexpression of any of the HDAC transcript analyzed was found in the

tumor tissues, as compared with corresponding normal tissues. However, while HDAC1 and HDAC2 mRNA levels were equivalent between matched normal and malignant prostate tissues, the transcript expression profiles of the other HDACs were more variable in the prostate samples. Indeed, a twofold lower level of HDAC3, HDAC4, HDAC5, HDAC6, HDAC7, HDAC8 mRNA expression was observed in several tumors as compared with their normal counterpart. In an effort to determine if this differential HDAC transcript expression between normal and malignant prostate tissues would translate into a similar altered HDAC expression at the protein level, we performed immunoblot and histochemistry experiments using different specific anti-HDAC antibodies. Because of the limited availability of antibodies that generated appropriate signals and/or stainings, our analysis mainly focused on the expression of HDAC1, HDAC5, and HDAC8.

Nuclear expression of HDAC1 was detected in the 3 human prostate cancer cell lines tested. These data are in accordance with previous findings indicating that HDAC1 is a predominantly nuclear protein with ubiquitous expression (Yang WM, Yao YL et al., 1997; Emiliani S, Fischle W et al., 1998; Hu E, Chen Z et al., 2000). Results from our immunoblot experiments performed on total protein extracts prepared from matched malignant and normal prostate tissues clearly showed that the abundance of HDAC1 protein was increased in the majority of cancer tissues as compared with their

normal counterpart. Searching for the precise distribution of HDAC1 in the different cell types present in the prostate gland, we unexpectedly observed that there was in fact no significant difference in nuclear HDAC1 levels between malignant and normal epithelial cells. Nevertheless, prostate stromal cells exhibited substantially lower amounts of the proteins than epithelial cells. Thus, since prostate cancer tissues are enriched with malignant epithelial cells, we hypothesized that HDAC1 overexpression in the cancer tissues, as assessed by immunoblot, merely reflected an increased epithelial/stromal cells ratio. Our explanation was validated by additional immunoblot experiments demonstrating that the levels of HDAC1 in the prostate tissues was significantly associated with the abundance of cytokeratin 18, a specific marker of prostate secretory epithelial cells. Similar experiments using human normal and malignant breast tissues showed i) no difference in HDAC1 expression between malignant and normal epithelial cells, ii) a reduced HDAC1 expression in stromal cells as compared with epithelial cells, and iii) a direct correlation between HDAC1 levels and the abundance of epithelial cells in breast tissues (*Waltregny D., unpublished observations*). Together, our data indicate that the importance of HDAC1 expression, and presumably deacetylase activity, displays variability among different cell types from the same organ.

Our findings are in disagreement with those from a previous report (Patra SK et al., 2001). Despite the use of the same anti-HDAC1 antibody (Ab2), Patra et al. found higher nuclear levels of HDAC1 in prostate cancer cells than in benign prostatic hyperplasia (Patra SK, Patra A et al., 2001). In our study, with the use of two different anti-HDAC1 antibodies applied to tissue sections harboring both non-malignant and malignant prostate cancer cells (Figures 4 and 5), we clearly demonstrate the absence of changes in HDAC1 abundance between the 2 cell types as well as between cancer lesions of various degree of differentiation. It is intriguing that in the report from Patra et al., the microphotographs of anti-HDAC1 immunostaining display either only adenocarcinoma cells or only benign glands. The alterations in HDAC levels observed by these authors might have been the result of differences in fixation time or tissue processing methods between the normal and cancer tissues analyzed.

In spite of the differences in HDAC1 protein levels between non-malignant and malignant tissue extracts

by immunoblot, our results from real time RT-PCR revealed no significant modulation in HDAC1 mRNA levels between those tissues. We also observed discordant mRNA and protein levels for HDAC1 and HDAC8 among the 3 prostate cancer cell lines tested, while the abundance of HDAC5 mRNA levels in those cell lines correlated with the protein levels of this enzyme. It has been suggested that HDAC1 protein could be degraded through the proteasome pathway in MCF-7 human breast cancer cells (Zhou Q, Melkounian ZK et al., 2000). It is possible that the rate of protein degradation of some HDACs is diversely regulated in different cell types. Further experiments, e.g. RNA in situ hybridization, would be required to address this point.

Likewise HDAC1, HDAC8, another class I HDAC, is thought to be ubiquitously expressed in the nucleus of mammalian cells although its pattern of transcript expression in various human tissues and cancer cell lines may differ from that of HDAC1 and HDAC3 (Buggy JJ, Sideris ML et al., 2000; Hu E, Chen Z et al., 2000; Van den Wyngaert I, de Vries W et al., 2000). It has been previously reported that HDAC8 mRNA can be detected in the normal prostate gland (Van den Wyngaert I, de Vries W et al., 2000). Hu et al. have reported that the sub-cellular distribution of over-expressed human HDAC8 in NIH-3T3 cells is mainly nuclear. However, van den Wyngaert et al. have shown that HDAC8 overexpression in HEK293 cells leads to its concentration in nuclear regions as well as in the cytosol (Van den Wyngaert I, de Vries W et al., 2000). In the present study, we found that HDAC1 and HDCA8 mRNA and protein expression profiles in the normal and cancerous prostate gland differed significantly. While HDAC1 protein was predominantly expressed in the nucleus of prostate epithelial cells, HDCA8 enzyme was mainly restricted to the cytoplasm of prostate stromal cells. On the basis of our immunohistochemistry results, and since, as already mentioned earlier, tumor samples are enriched with epithelial cells, it was not surprising that our immunoblot analysis of HDAC8 expression showed a relative decrease in the abundance of the enzyme in protein extracts from tumor samples as compared with normal ones. Thus, the expression profiles of two class I HDACs, HDAC1 and HDAC8, in prostate tissues are distinctly different, suggesting different biological functions for these enzymes. Our findings also point to an unexpected sub-cellular localization of HDAC8. It has been reported that

HDAC3, another class I HDAC, can also be localized in the nucleus and the cytosol (Yang WM et al., 2002). The precise role of these two HDACs in each cellular compartment is at present unknown. One may hypothesize that, besides their histone deacetylase activity in the nucleus, these enzymes may act on different substrates in the cytoplasm. In fact, it has been recently shown that HDAC6 can deacetylate  $\alpha$ -tubulin, a cytoskeletal protein present in the cytosol (Hubbert C, Guardiola A et al., 2002; Matsuyama A et al., 2002).

The expression levels of class II HDACs in human tissues are more variable than those of class I enzymes (Grozingier CM, Hassig CA et al., 1999). HDAC5, a class II HDAC, is involved in skeletal muscle growth and differentiation (Lu J et al., 2000a; Lu J et al., 2000b) and its transcript is primarily expressed in skeletal muscle, heart, brain, and placenta (Grozingier CM, Hassig CA et al., 1999; Verdel A and Khochbin S, 1999). In the human prostate gland, HDAC5 mRNA expression was detectable, though at much lower levels than that of HDAC1. Furthermore, while HDAC5 protein was expressed in the 3 prostate cancer cell lines, we did not detect the protein in the human prostate tissues by immunoblot, suggesting that this class II HDAC is either not expressed or expressed at a very low level in the prostate.

In conclusion, our data indicate that several HDACs display distinct cell type and sub-cellular compartment expression profiles in the prostate gland, suggesting specific biological functions for these enzymes. Our findings also emphasize on the careful interpretation required to analyze expression data generated with the use of total protein extracts from human tissues, unless in situ detection of the protein(s) of interest is performed.

### Funding

*National Fund for Scientific Research (Belgium), Centre Anti-Cancéreur de l'Université de Liège, Fondation Léon Frédéricq, TELEVIE, Interuniversity Attraction Pole #P5/31, STROMA FP6 #503233 and Roche Diagnostics (Penzberg, Germany).*

### References

- Alland L, Muhle R, Hou H Jr, Potes J, Chin L, Schreiber-Agus Net al. Role for N-CoR and histone deacetylase in Sin3-mediated transcriptional repression. *Nature* 1997;387:49-55.
- Bartl S, Taplick J, Lagger G, Khier H, Kuchler K, Seiser C. Identification of mouse histone deacetylase 1 as a growth factor-inducible gene. *Mol Cell Biol* 1997;17:5033-43.
- Buggy JJ, Sideris ML, Mak P, Lorimer DD, McIntosh B, Clark JM. Cloning and characterization of a novel human histone deacetylase, HDAC8. *Biochem J* 2000;350:199-205.
- Butler LM, Agus DB, Scher HI, Higgins B, Rose A, Cordon-Cardo C, et al. Suberoylanilide hydroxamic acid, an inhibitor of histone deacetylase, suppresses the growth of prostate cancer cells in vitro and in vivo. *Cancer Res* 2000;60:5165-5170.
- Butler LM, Webb Y, Agus DB, Higgins B, Tolentino TR, Kutko MC, et al. Inhibition of transformed cell growth and induction of cellular differentiation by pyroxamide, an inhibitor of histone deacetylase. *Clin Cancer Res* 2001;7:962-970.
- Cress WD, Seto E. Histone deacetylases, transcriptional control, and cancer. *J Cell Physiol* 2000;184:1-16.
- Dangond F, Henriksson M, Zardo G, Caiafa P, Ekstrom TJ, Gray SG. Differential expression of class I HDACs: roles of cell density and cell cycle. *Int J Oncol* 2001;19:773-7.
- De Ruijter AJ, Van Gennip AH, Caron HN, Kemp S, Van Kuilenburg AB. Histone deacetylases (HDACs): characterization of the classical HDAC family. *Biochem J* 2003;370:737-49.
- Deroanne CF, Bonjean K, Servotte S, Devy L, Colige A, Clausse N, et al. Histone deacetylase inhibitors as anti-angiogenic agents altering vascular endothelial growth factor signaling. *Oncogene* 2002;21:427-36.
- Ellerhorst J, Nguyen T, Cooper DN, Estrov Y, Lotan D, Lotan R. Induction of differentiation and apoptosis in the prostate cancer cell line LNCaP by sodium butyrate and galectin-1. *Int J Oncol* 1999;14:225-32.
- Emiliani S, Fischle W, Van Lind C, Al-Abed Y, Verdin E. Characterization of a human RPD3 ortholog, HDAC3. *Proc Natl Acad Sci USA* 1998;95:2795-800.
- Fink L, Seeger W, Ermert L, Hanze J, Stahl U, Grimminger F, et al. Real-time quantitative RT-PCR after laser-assisted cell picking. *Nat Med* 1998;4:1329-33.
- Fischer DD, Cai R, Bhatia U, Asselbergs FA, Song C, Terry R, et al. Isolation and Characterization of a novel class II Histone Deacetylase, HDAC10. *J Biol Chem* 2002;277:6656-66.
- Fischle W, Dequiedt F, Hendzel MJ, Guenther MG, Lazar MA, Voelter W et al. Enzymatic activity associated with class II HDACs is dependent on a multiprotein complex containing HDAC3 and SMRT/N-CoR. *Mol Cell* 2002;9:45-57.
- Frye RA. Characterization of five human cDNAs with homology to the yeast SIR2 gene: Sir2-like proteins (sirtuins) metabolize NAD and may have protein ADP-ribosyltransferase activity. *Biochem Biophys Res Commun* 1999;260:273-9.
- Gao L, Cueto MA, Asselbergs F, Atadja P. Cloning and functional characterization of HDAC11, a novel member of the human histone deacetylase family. *J Biol Chem* 2002;277:25748-55.
- Gleason DF, Mellinger GT. Prediction of prognosis for prostatic adenocarcinoma by combined histological grading and clinical staging. *J Urol* 1974;111:58-64.
- Gleave ME, Sato N, Sadar M, Yago V, Bruchovsky N, Sullivan L. Butyrate analogue, isobutyramide, inhibits tumor growth and time to androgen-independent progression in the human prostate LNCaP tumor model. *J Cell Biochem* 1998;69:271-81.
- Gray SG, Ekstrom TJ. Effects of cell density and trichostatin A on the expression of HDAC1 and p57Kip2 in Hep 3B cells. *Biochem Biophys Res Commun* 1998;245:423-7.
- Gray SG, Ekstrom TJ. The human histone deacetylase family. *Exp Cell Res* 2001;262:75-83.
- Grozingier CM, Hassig CA, Schreiber SL. Three proteins define a class of human histone deacetylases related to yeast Hda1p. *Proc Natl Acad Sci USA* 1999;96:4868-73.
- Grunstein M. Histone acetylation in chromatin structure and transcription. *Nature* 1997;389:349-52.
- Guardiola AR, Yao TP. Molecular Cloning and Characterization of a Novel Histone Deacetylase HDAC10. *J Biol Chem* 2002;277:33506.
- Halgunset J, Lamvik T, Espevik T. Butyrate effects on growth, morphology, and fibronectin production in PC-3 prostatic carcinoma cells. *Prostate* 1988;12:65-77.
- Halkidou K, Cook S, Leung HY, Neal DE, Robson CN. Nuclear accumulation of histone deacetylase 4 coincides with the loss of androgen sensitivity in hormone refractory cancer of the prostate. *Eur*

- Urol 2004; in press.
- Hu E, Chen Z, Fredrickson T, Zhu Y, Kirkpatrick R, Zhang GF, Johanson K, et al. Cloning and characterization of a novel human class I histone deacetylase that functions as a transcription repressor. *J Biol Chem* 2000;275:15254-64.
- Hubbert C, Guardiola A, Shao R, Kawaguchi Y, Ito A, Nixon A, et al. HDAC6 is a microtubule-associated deacetylase. *Nature* 2002;417:455-8.
- Imai S, Armstrong CM, Kaeberlein M, Guarente L. Transcriptional silencing and longevity protein Sir2 is an NAD-dependent histone deacetylase. *Nature* 2000;403:795-800.
- Kao HY, Downes M, Ordentlich P, Evans RM. Isolation of a novel histone deacetylase reveals that class I and class II deacetylases promote SMRT-mediated repression. *Genes Dev* 2000;14:55-66.
- Kao HY, Lee CH, Komarov A, Han CC, Evans RM. Isolation and characterization of mammalian HDAC10, a novel histone deacetylase. *J Biol Chem* 2002;277:187-93.
- Kim MS, Kwon HJ, Lee YM, Baek JH, Jang JE, Lee SW, et al. Histone deacetylases induce angiogenesis by negative regulation of tumor suppressor genes. *Nat Med* 2001;7:437-43.
- Kim YB, Lee KH, Sugita K, Yoshida M, Horinouchi S. Oxamflatin is a novel antitumor compound that inhibits mammalian histone deacetylase. *Oncogene* 1999;18:2461-70.
- Knoepfler PS, Eisenman RN. Sin meets NuRD and other tails of repression. *Cell* 1999;99:447-50.
- Koipally J, Renold A, Kim J, Georgopoulos K. Repression by Ikaros and Aiolos is mediated through histone deacetylase complexes. *Embo J* 1999;18:3090-100.
- Kramer OH, Gottlicher M, Heinzel T. Histone deacetylase as a therapeutic target. *Trends Endocrinol Metab* 2001;12:294-300.
- Kuefer R, Hofer MD, Altug V, Zorn C, Genze F, Kunzi-Rapp K, et al. Sodium butyrate and tributyrin induce in vivo growth inhibition and apoptosis in human prostate cancer. *British Journal of Cancer* 2004;535-41.
- Kwon HJ, Owa T, Hassig CA, Shimada J, Schreiber SL. Depudecin induces morphological reversion of transformed fibroblasts via the inhibition of histone deacetylase. *Proc Natl Acad Sci USA* 1998;95:3356-61.
- Langley E, Pearson M, Faretta M, Bauer UM, Frye RA, Minucci S, et al. Human SIR2 deacetylates p53 and antagonizes PML/p53-induced cellular senescence. *Embo J* 2002;21:2383-96.
- Lu J, McKinsey TA, Nicol RL, Olson EN. Signal-dependent activation of the MEF2 transcription factor by dissociation from histone deacetylases. *Proc Natl Acad Sci U S A* 2000a;97:4070-5.
- Lu J, McKinsey TA, Zhang CL, Olson EN. Regulation of skeletal myogenesis by association of the MEF2 transcription factor with class II histone deacetylases. *Mol Cell* 2000b;6:233-44.
- Luo J, Nikolaev AY, Imai S, Chen D, Su F, Shiloh A, et al. Negative control of p53 by Sir2 $\alpha$  promotes cell survival under stress. *Cell* 2001;107:137-48.
- Maier S, Reich E, Martin R, Bachem M, Altug V, Hautmann RE, et al. Tributyrin induces differentiation, growth arrest and apoptosis in androgen-sensitive and androgen-resistant human prostate cancer cell lines. *Int J Cancer* 2000;88:245-51.
- Marks PA, Richon VM, Rifkind RA. Histone deacetylase inhibitors: inducers of differentiation or apoptosis of transformed cells. *J Natl Cancer Inst* 2000;92:1210-6.
- Matsuyama A, Shimazu T, Sumida Y, Saito A, Yoshimatsu Y, Seigneurin-Berny D, et al. In vivo destabilization of dynamic microtubules by HDAC6-mediated deacetylation. *Embo J* 2002;21:6820-31.
- Megee PC, Morgan BA, Mittman BA, Smith MM. Genetic analysis of histone H4: essential role of lysines subject to reversible acetylation. *Science* 1990;247:841-5.
- Nagy L, Kao HY, Chakravarti D, Lin RJ, Hassig CA, Ayer DE, et al. Nuclear receptor repression mediated by a complex containing SMRT, mSin3A, and histone deacetylase. *Cell* 1997;89:373-80.
- Patra SK, Patra A, Dahiya R. Histone deacetylase and DNA methyltransferase in human prostate cancer. *Biochem Biophys Res Commun* 2001;287:705-13.
- Pili R, Kruszewski MP, Hager BW, Lantz J, Carducci MA. Combination of phenylbutyrate and 13-cis retinoic acid inhibits prostate tumor growth and angiogenesis. *Cancer Res* 2001;61:1477-85.
- Rennie PS, Nelson CC. Epigenetic mechanisms for progression of prostate cancer. *Cancer Metastasis Rev* 1998;17:401-9.
- Schröder FH, Hermanek P, Denis L, Fair WR, Gospodarowicz MK, Pavone-Macaluso M. The TNM classification of prostate cancer. *The Prostate* 1992;4:129-38.
- Schwer B, North BJ, Frye RA, Ott M, Verdin E. The human silent information regulator (Sir)2 homologue hSIRT3 is a mitochondrial nicotinamide adenine dinucleotide-dependent deacetylase. *J Cell Biol* 2002;158:647-57.
- Signoretti S, Waltregny D, Dilks J, Isaac B, Lin D, Garraway L, et al. p63 is a prostate basal cell marker and is required for prostate development. *Am J Pathol* 2000;157:1769-75.
- Suenaga M, Soda H, Oka M, Yamaguchi A, Nakatomi K, Shiozawa K, et al. Histone deacetylase inhibitors suppress telomerase reverse transcriptase mRNA expression in prostate cancer cells. *Int J Cancer* 2002;97:621-5.
- Taunton J, Hassig CA, Schreiber SL. A mammalian histone deacetylase related to the yeast transcriptional regulator Rpd3p. *Science* 1996;272:408-11.
- Tong JJ, Liu J, Bertos NR, Yang XJ. Identification of HDAC10, a novel class II human histone deacetylase containing a leucine-rich domain. *Nucleic Acids Res* 2002;30:1114-23.
- Van den Wyngaert I, de Vries W, Kremer A, Neefs J, Verhasselt P, Luyten WH, et al. Cloning and characterization of human histone deacetylase 8. *FEBS Lett* 2000;478:77-83.
- Vaziri H, Dessain SK, Ng Eaton E, Imai SI, Frye RA, Pandita TK, et al. hSIR2(SIRT1) functions as an NAD-dependent p53 deacetylase. *Cell* 2001;107:149-59.
- Verdel A, Khochbin S. Identification of a new family of higher eukaryotic histone deacetylases. Coordinate expression of differentiation-dependent chromatin modifiers. *J Biol Chem* 1999;274:2440-5.
- Walls R, Thibault A, Liu L, Wood C, Kozlowski JM, Figg WD, et al. The differentiating agent phenylacetate increases prostate-specific antigen production by prostate cancer cells. *Prostate* 1996;29:177-82.
- Wheeler TM, Lebovitz RM. Fresh tissue harvest for research from prostatectomy specimens. *Prostate* 1994;25:274-9.
- Yang WM, Tsai SC, Wen YD, Fejer G, Seto E. Functional domains of histone deacetylase-3. *J Biol Chem* 2002;277:9447-54.
- Yang WM, Yao YL, Sun JM, Davie JR, Seto E. Isolation and characterization of cDNAs corresponding to an additional member of the human histone deacetylase gene family. *J Biol Chem* 1997;272:28001-7.
- Zhou Q, Melkoudian ZK, Lucktong A, Moniwa M, Davie JR, Strobl JS. Rapid induction of histone hyperacetylation and cellular differentiation in human breast tumor cell lines following degradation of histone deacetylase-1. *J Biol Chem* 2000;275:35256-63.
- Zhou X, Marks PA, Rifkind RA, Richon VM. Cloning and characterization of a histone deacetylase, HDAC9. *Proc Natl Acad Sci USA* 2001;98:10572-7.